Transverse vibration of nematic elastomer Timoshenko beams

Dong Zhao, Ying Liu,* and Chuang Liu
Department of Mechanics, School of Civil Engineering, Beijing Jiaotong University, Beijing 100044, China
(Received 8 September 2016; revised manuscript received 17 November 2016; published 18 January 2017)

Being a rubber-like liquid crystalline elastomer, a nematic elastomer (NE) is anisotropic viscoelastic, and displays dynamic soft elasticity. In this paper, the transverse vibration of a NE Timoshenko beam is studied based on the linear viscoelasticity theory of nematic elastomers. The governing equation of motion for the transverse vibration of a NE Timoshenko beam is derived. A complex modal analysis method is used to obtain the natural frequencies and decrement coefficients of NE beams. The influences of the nematic director rotation, the rubber relaxation time, and the director rotation time on the vibration characteristic of NE Timoshenko beams are discussed in detail. The sensitivity of the dynamic performance of NE beams to director initial angle and relaxation times provides a possibility of intelligent controlling of their dynamic performance.

DOI: 10.1103/PhysRevE.95.012703

I. INTRODUCTION

Nematic elastomers are one kind of new materials that simultaneously combine the orientational properties of liquid crystals and the elastic properties of rubbers. Microscopically, a nematic elastomer (NE) has a structure constructed by long polymer molecules and chains, the main stable elements with a common direction vector or director [1]. The polymer network is connected by transverse links between the ends of molecules. These links allow the rotations of individual molecules like ball pivots [2,3]. From the mechanical viewpoint, this means that a NE is strongly anisotropic on the macro level, and in addition to the traditional strains, it might have additional rotational degrees of freedom. Therefore, NEs display a soft elasticity characterized by vanishing shear stresses for a range of longitudinal strains applied perpendicular to the nematic direction, which results in large deformations under small applied forces [3–5]. In addition to their unusual static properties, NEs also display novel dynamic properties. It is found that an internal relaxation of the nematic director leads to a dynamic mechanical softening of NEs, that is, dynamic soft elasticity [6–10]. What is more, nematic elastomers have novel responses to external stimuli, such as electric fields, temperature, and light. These properties of soft matter have attracted increasing interest of researchers in the fields of microelectronics, biomechanics (actuators or artificial muscles), and nanomechanics in the context of a possible nontraditional matrix. Adequate modeling of NEs becomes an important issue for prospective applications in crucial fields.

Recently, more and more works have been done to investigate the dynamic mechanical performance of nematic elastomers. Terentjev and Warner [5,11] developed a linear viscoelastic theory of liquid crystal elastomers in a hydrodynamic (low-frequency) limit. Then, on the basis of linear viscoelastic theory, Fradkin *et al.* [12] studied the acoustic waves in nematic elastomers under a low frequency. Singh [13] studied the reflection of homogeneous elastic waves from the free surface of a nematic elastomer half space. Zakharov [14] studied the properties of surface and edge waves in solids with a nematic coating. Yang *et al.* [15] investigated Rayleigh wave propagation in nematic elastomers. Jin *et al.* [16] studied the light-induced nonhomogeneity and gradient bending of a photochromic liquid crystal elastomer (LCE) beam, and proposed a gradient model for the light-induced bending of a photochromic LCE beam and its nonlinear behaviors, considering the optochemical process and the nematic-isotropic phase transition [17]. Warner [18] studied the mechanical and optical bending of nematic elastomer cantilevers. Li *et al.* [19] modeled the transient temperature distribution and the bending kinetics of a liquid crystal elastomer cantilever under the radiation of a laser diode (LD) light. Ábrahám *et al.* [20] presented a dimensionless parametric study of nematic photoelastomer beams under the combined effects of light and mechanical loads to show how the number of stress-free layers depends on the dimensionless parameters. An *et al.* [21] described a finite element method (FEM) to model the buckling of a constrained LCE beam working as a valve for microfluidic flow when heated. Li *et al.* [22] studied the light-driven bending vibration of a liquid crystal elastomer cantilever beam.

It is seen that these works to some extent exhibit the dynamic behavior of nematic elastomers and the properties of nematic elastomers in external stimuli. However, different from the general viscoelastic materials, the existence of the director as well as the director rotation definitely leads to particular behavior of NE structures. More investigation should be carried out to further disclose the dynamic responses of nematic elastomer structures for the purpose of the structural design based on nematic elastomers. In this paper, the transverse vibration of a nematic elastomer beam is investigated based on the viscoelastic theory in the hydrodynamic limit and Timoshenko beam theory. The governing equation for the transverse vibration of a Timoshenko nematic elastomer beam is derived. The influence of the nematic director, the rubber relaxation time, and the director rotation time on the vibration properties of nematic elastomer beam is discussed. Finally, the conclusion is given.

II. THE VISCOELASTIC CONSTITUTIVE RELATION OF NEMATIC ELASTOMERS

Figure 1 gives a diagrammatic sketch of NE structures and director rotation. In fact, the linear viscoelasticity of nematic elastomers has been well studied. The governing equations

*yliu5@bjtu.edu.cn

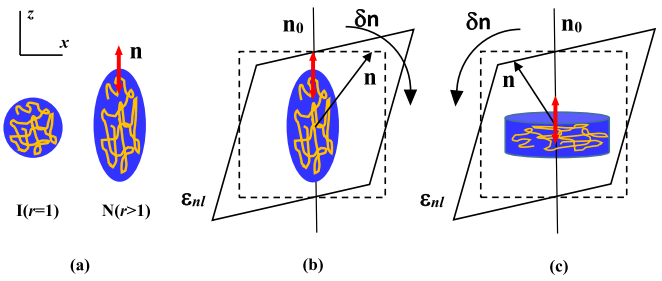

FIG. 1. Diagrammatic sketch of nematic elastomers: (a) microscopic picture: polymers are average spherical in the isotropic state (I) and elongated in the nematic state (N); the director $\mathbf{n}$ points along the long axis of the shape spheroid; (b) director rotation in prolate elastomers (the long axis of the spheroid points along the nematic director $\mathbf{n}$) toward the elongation diagonal direction; (c) director rotation in oblate elastomers (the long axis of the spheroid is perpendicular to the nematic director $\mathbf{n}$) toward the compression direction; in order to distinguish the director after rotation from the director before rotation, the initial state of the director is marked as $\mathbf{n}_0$; ε_{nl} is the symmetric shear strain and $\delta\mathbf{n}$ is the variation of director orientation due to the shear strain.

have been proposed by Terentjev *et al.* [11] and Fradkin *et al.* [12] by applying the variation principle to the Lagrangian density amended by the Rayleigh dissipation function, that is, $\mathcal{L} - T\dot{S} = \rho\dot{\mathbf{u}}^2/2 - F(\mathbf{u},\Theta) - T\dot{S}(\dot{\mathbf{u}},\dot{\Theta})$, with independent variables $\mathbf{u}$ and Θ.

Here the elastic potential energy density in a solid takes the form

$$\begin{aligned} F &= c_1(\mathbf{n}\cdot\tilde{\boldsymbol{\varepsilon}}\cdot\mathbf{n})^2 + 2c_2\mathrm{tr}[\dot{\boldsymbol{\varepsilon}}](\mathbf{n}\cdot\tilde{\boldsymbol{\varepsilon}}\cdot\mathbf{n}) + c_3(\mathrm{tr}[\boldsymbol{\varepsilon}])^2 \\ &\quad + 2c_4[(\mathbf{n}\times\tilde{\boldsymbol{\varepsilon}})\times\mathbf{n}]^2 + 4c_5[\mathbf{n}\times(\tilde{\boldsymbol{\varepsilon}}\cdot\mathbf{n})]^2 \\ &\quad + \tfrac{1}{2}d_1[\mathbf{n}\times\Theta]^2 + d_2\mathbf{n}\cdot\tilde{\boldsymbol{\varepsilon}}\cdot[\mathbf{n}\times\Theta], \end{aligned} \tag{1}$$

and the Rayleigh dissipation function (entropy production density) is a quadratic form of the corresponding velocities

$$\begin{aligned} T\dot{S} &= a_1(\mathbf{n}\cdot\dot{\tilde{\boldsymbol{\varepsilon}}}\cdot\mathbf{n})^2 + 2a_2\mathrm{tr}[\dot{\boldsymbol{\varepsilon}}](\mathbf{n}\cdot\dot{\tilde{\boldsymbol{\varepsilon}}}\cdot\mathbf{n}) + a_3(\mathrm{tr}[\dot{\boldsymbol{\varepsilon}}])^2 \\ &\quad + 2a_4[(\mathbf{n}\times\dot{\tilde{\boldsymbol{\varepsilon}}})\times\mathbf{n}]^2 + 4a_5[\mathbf{n}\times(\dot{\tilde{\boldsymbol{\varepsilon}}}\cdot\mathbf{n})]^2 \\ &\quad + \tfrac{1}{2}\gamma_1[\mathbf{n}\times\dot{\Theta}]^2 + \gamma_2\mathbf{n}\cdot\dot{\tilde{\boldsymbol{\varepsilon}}}\cdot[\mathbf{n}\times\dot{\Theta}], \end{aligned} \tag{2}$$

where $\mathbf{u}$ is the displacement vector, $\tilde{\boldsymbol{\varepsilon}}$ is the deviator of the symmetrical strain tensor $\boldsymbol{\varepsilon}$, $\Omega = \nabla\times\mathbf{u}/2$ is the shear induced local rotation angle of rubber, $\delta\mathbf{n}$ is a small variation in the undistorted nematic director due to the shear strain, and $\Theta = \Omega - [\mathbf{n}\times\delta\mathbf{n}]$ denotes the difference between the local rotation angle and the rotation angle of the director $[\mathbf{n}\times\delta\mathbf{n}]$. The stiffness set c_i corresponds to the transversal isotropy with the direction $\mathbf{n}$ along axis z. T is the temperature and S the entropy; a_i are viscous coefficients. d_i denotes the rotational stiffness with the relations for the relaxation times $a_i = c_i\tau_R$, $\gamma_1 = d_1\tau_1$, and $\gamma_2 = d_2\tau_2$. In principle, the relaxation times for various a_i will differ, and they also differ from τ_1 and τ_2. However, there is a significant separation between these two groups of characteristic time scales, that is, between the polymer-specific Rouse time scale τ_R, and τ_1, τ_2. The director rotation time, τ_1, has been identified by Terentjev and Warner [11] and experimentally measured as 10^{-1} to 10^{-2} s [23,24]. In contrast, the characteristic time of rubber relaxation τ_R is much shorter, of the order of the Rouse time of the corresponding polymer chains, which can be as low as 10^{-5} to 10^{-6} s. Accordingly, the small differences between the values of τ_R for different deformation modes are ignored. Moreover, due to the demand on positive definiteness of the Rayleigh function, that is, Eq. (2), it follows that a constraint $\gamma_2^2 \leqslant 8a_5\gamma_1$ should be maintained, and consequently we have $\tau_2^2 \leqslant 8c_5d_1\tau_R\tau_1/d_2^2$.

By applying the variation principle to the combined Lagrangian and Rayleigh function with respect to their variables (coordinates and corresponding velocities), the governing equations of motion of viscous nematic solids are obtained by neglecting the effects of Frank elasticity on the director gradient, that is,

$$\begin{aligned} \rho\ddot{\mathbf{u}} &= \nabla\cdot\boldsymbol{\sigma}, \\ \mathbf{n}\times[(d_1+\gamma_1\partial_t)\mathbf{n}\times\Theta + (d_2+\gamma_2\partial_t)\mathbf{n}\cdot\boldsymbol{\varepsilon}] &= 0. \end{aligned} \tag{3}$$

When we choose the z axis to lie in the undistorted director $\mathbf{n}$, the components of the viscoelastic stress tensor $\boldsymbol{\sigma}$ take the form

$$\begin{aligned} \sigma_{xx} &= (1+\tau_R\partial_t)(C_{11}\varepsilon_{xx} + C_{12}\varepsilon_{yy} + C_{13}\varepsilon_{zz}), \\ \sigma_{yy} &= (1+\tau_R\partial_t)(C_{12}\varepsilon_{xx} + C_{11}\varepsilon_{yy} + C_{13}\varepsilon_{zz}), \\ \sigma_{zz} &= (1+\tau_R\partial_t)(C_{13}\varepsilon_{xx} + C_{13}\varepsilon_{yy} + C_{33}\varepsilon_{zz}), \\ \sigma_{yz} &= 2(1+\tau_R\partial_t)C_{44}\varepsilon_{yz} + d_2(1+\tau_2\partial_t)\Theta_1/2, \\ \sigma_{xz} &= 2(1+\tau_R\partial_t)C_{44}\varepsilon_{xz} - d_2(1+\tau_2\partial_t)\Theta_2/2, \\ \sigma_{xy} &= 2(1+\tau_R\partial_t)C_{66}\varepsilon_{xy}, \end{aligned} \tag{4}$$

with

$$\begin{aligned} C_{11} &= \tfrac{2}{9}c_1 - \tfrac{4}{3}c_2 + 2c_3 + \tfrac{20}{9}c_4, \\ C_{12} &= \tfrac{2}{9}c_1 - \tfrac{4}{3}c_2 + 2c_3 - \tfrac{16}{9}c_4, \\ C_{13} &= -\tfrac{4}{9}c_1 + \tfrac{2}{3}c_2 + 2c_3 - \tfrac{4}{9}c_4, \\ C_{33} &= \tfrac{8}{9}c_1 + \tfrac{8}{3}c_2 + 2c_3 + \tfrac{8}{9}c_4, \\ C_{44} &= 2c_5, \quad C_{66} = \tfrac{1}{2}(C_{11} - C_{12}) = 2c_4. \end{aligned} \tag{5}$$

The elastic constant c_3 is dominated by the bulk modulus B and $c_3 = B/2$ [12]. The bulk modulus is independent of the configurational entropy of the polymer chains and determined by molecular forces resisting the compression of a liquid, which results in B of approximately 10^9 to 10^{10} Pa, much greater than the typical value of rubber modulus, μ_0, which is around 10^5 Pa [12].

In order to seek the solutions of the displacement in the usual form $\mathbf{u} = \mathbf{u}^* e^{-i\omega t}$ [25], where $\mathbf{u}^*$ is the amplitude vector and ω is frequency, the effective stress $\boldsymbol{\sigma}$ is rewritten in the following form:

$$\begin{bmatrix} \sigma_{xx} \\ \sigma_{yy} \\ \sigma_{zz} \\ \sigma_{yz} \\ \sigma_{xz} \\ \sigma_{xy} \end{bmatrix} = (1 - i\omega\tau_R) \begin{bmatrix} C_{11} & C_{12} & C_{13} & 0 & 0 & 0 \\ C_{12} & C_{11} & C_{13} & 0 & 0 & 0 \\ C_{13} & C_{13} & C_{33} & 0 & 0 & 0 \\ 0 & 0 & 0 & 2C_{44}^R & 0 & 0 \\ 0 & 0 & 0 & 0 & 2C_{44}^R & 0 \\ 0 & 0 & 0 & 0 & 0 & 2C_{66} \end{bmatrix} \begin{bmatrix} \varepsilon_{xx} \\ \varepsilon_{yy} \\ \varepsilon_{zz} \\ \varepsilon_{yz} \\ \varepsilon_{xz} \\ \varepsilon_{xy} \end{bmatrix}, \tag{6}$$

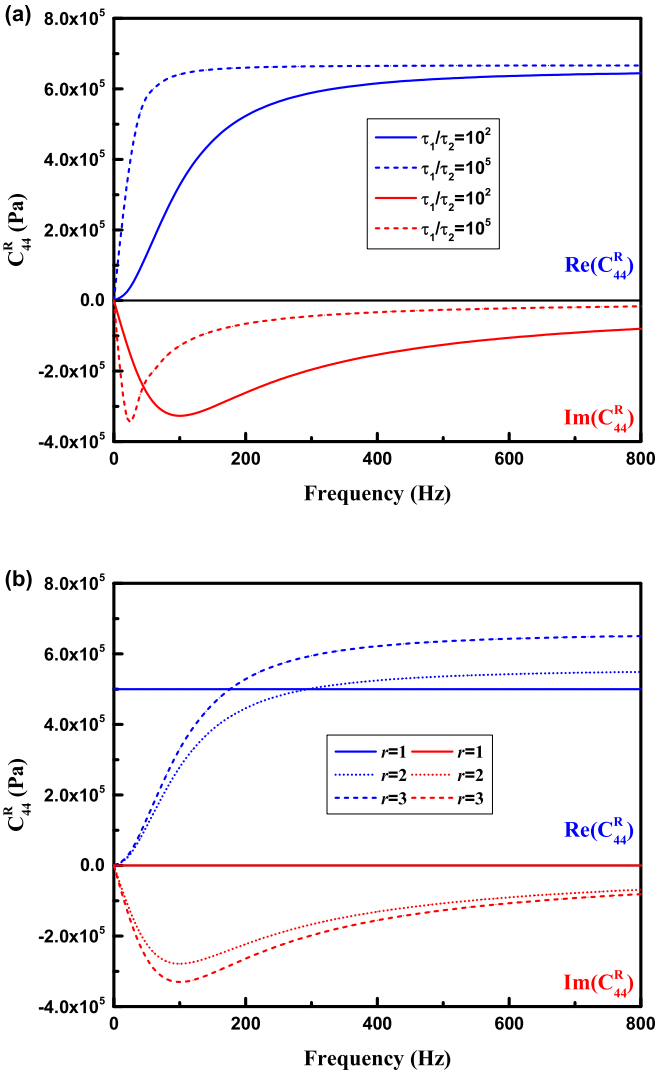

FIG. 2. The relationship between the renormalized shear modulus and the frequencies (a) for different τ_1/τ_2 with $r = 3$, $\tau_2 = 10^{-4}$ s, $\tau_R = 10^{-5}$ s; and (b) for different r with $\tau_1 = 10^{-2}$ s, $\tau_2 = 10^{-4}$ s, $\tau_R = 10^{-5}$ s. The blue lines represent the real part of C_{44}^R and the red lines represent the imaginary part of C_{44}^R.

where the effective transversal stresses have a nonclassical form with the renormalized shear modulus,

$$C_{44}^R = 2c_5 - \frac{d_2^2}{4d_1}\frac{(1-i\omega\tau_2)^2}{(1-i\omega\tau_1)(1-i\omega\tau_R)}. \tag{7}$$

It can be seen that the renormalized shear modulus is frequency dependent. Besides, c_5, d_1, and d_2 are all related to the chain anisotropic parameter r ($r = l_\parallel/l_\perp$ measures the anisotropy of the average chain shape spheroid, that is, the deviation from a sphere; $l_\parallel$ and $l_\perp$ are the effective lengths of steps in the directions parallel and perpendicular to director $\mathbf{n}$). Then Fig. 2 plots the relationship between the renormalized shear modulus C_{44}^R and the frequencies with different τ_1/τ_2 and r. The blue lines are the real part of C_{44}^R which are called storage moduli, and the red lines are the imaginary part of C_{44}^R which are called loss moduli. The storage modulus defines the amount of elastic energy stored in the material and the loss modulus

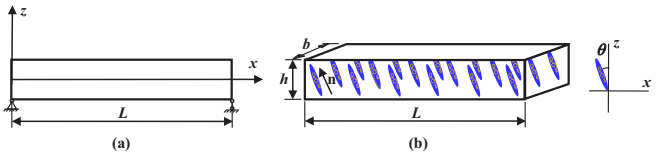

FIG. 3. The diagrammatic sketch of (a) a Timoshenko beam made of nematic elastomers; and (b) the undistorted director $\mathbf{n}$ having an initial angle θ with the z axis (θ is positive while it is counterclockwise).

is directly related to the viscous dissipation [5]. It is seen that the real part of C_{44}^R increases quickly from zero and then tends to a constant value with the further increasing of frequencies. For the imaginary part of C_{44}^R, it first decreases significantly along with the increase of the frequency, while after a critical transition frequency, the imaginary part of C_{44}^R is increased. When frequency gets to a certain value, the imaginary part of C_{44}^R tends to a stable value, and NEs reach a rubber plateau. This stable value is dependent on τ_1/τ_2, but if the frequency is large enough, it may approach zero. The nematic elastomers display dynamic soft elasticity at low frequency, and there is a transition from a liquid crystal response at a relatively low frequency to a rubber performance at a relatively high frequency. In Fig. 2(a), the larger the value of τ_1/τ_2 is, the smaller the critical transition frequency will be, and the larger the stable value is. As shown in Fig. 2(b), when $r = 1$, the real part of C_{44}^R is a constant and the imaginary part of C_{44}^R is zero, which corresponds to the pure isotropic viscoelastic material. When $r > 1$, bigger r leads to larger absolute values of the real and imaginary parts of C_{44}^R, while it has no effect on the critical transition frequencies.

Considering the plane-section assumption for beam theory, the effective stress $\boldsymbol{\sigma}$ can be simplified as

$$\begin{bmatrix}\sigma_{xx}\\ \sigma_{zz}\\ \sigma_{xz}\end{bmatrix} = (1-i\omega\tau_R)\begin{bmatrix}C_{11} & C_{13} & 0\\ C_{13} & C_{33} & 0\\ 0 & 0 & C_{44}^R\end{bmatrix}\begin{bmatrix}\varepsilon_{xx}\\ \varepsilon_{zz}\\ \gamma_{xz}\end{bmatrix}. \tag{8}$$

When the direction of the undistorted director $\mathbf{n}$ has an initial angle θ with z axis at an initial undeformed state (shown in Fig. 3), the effective stress $\boldsymbol{\sigma}$ is

$$\begin{bmatrix}\sigma_{xx}\\ \sigma_{zz}\\ \sigma_{xz}\end{bmatrix} = (1-i\omega\tau_R)\mathbf{T}^{-1}\begin{bmatrix}C_{11} & C_{13} & 0\\ C_{13} & C_{33} & 0\\ 0 & 0 & C_{44}^R\end{bmatrix}(\mathbf{T}^{-1})^T\begin{bmatrix}\varepsilon_{xx}\\ \varepsilon_{zz}\\ \gamma_{xz}\end{bmatrix}, \tag{9}$$

where

$$\mathbf{T} = \begin{bmatrix}\cos^2\theta & \sin^2\theta & 2\sin\theta\cos\theta\\ \sin^2\theta & \cos^2\theta & -2\sin\theta\cos\theta\\ -\sin\theta\cos\theta & \sin\theta\cos\theta & \cos^2\theta-\sin^2\theta\end{bmatrix}. \tag{10}$$

III. GOVERNING EQUATION OF MOTION FOR THE NEMATIC ELASTOMER BEAM

Due to the special properties, nematic elastomers have been exploited for a wide spectrum of applications, such as actuators, motors, and device applications. A very interesting example is that they can be used in artificial muscles [26]. A

beamlike structure made of nematic elastomers is an applicable model of an artificial muscle. As seen as Fig. 3, the undistorted director **n** has an initial angle θ with the z axis. Based on the Timoshenko beam theory, the displacements of an arbitrary point in the beam along the x, y, and z axes can be written as

$$\begin{aligned}\tilde{U}(x,z,t) &= z\phi(x,t),\\ \tilde{V}(x,z,t) &= 0,\\ \tilde{W}(x,z,t) &= w(x,t),\end{aligned} \tag{11}$$

where $w(x,t)$ is the transverse displacement at the neutral axis of the beam, $\phi(x,t)$ is the rotation of the cross section, and t is time. Employing the plane-section assumption, the formulas of the strain for a Timoshenko beam are given as

$$\begin{aligned}\varepsilon_{xx} &= z\frac{\partial\phi}{\partial x},\\ \varepsilon_{yy} &= \varepsilon_{zz} = \varepsilon_{xy} = \varepsilon_{yz} = 0,\\ \gamma_{xz} &= \frac{\partial w}{\partial x} + \phi,\end{aligned} \tag{12}$$

where ε_{xx} is the axial strain and γ_{xz} is the shear strain.

Then according to Eq. (9), we have

$$\begin{aligned}\sigma_{xx} = (1 - i\omega\tau_R)\{&\big[4C_{44}^R\sin^2\theta\cos^2\theta\\ &+ (C_{11}\cos^2\theta + C_{13}\sin^2\theta)\cos^2\theta\\ &+ \sin^2\theta(C_{13}\cos^2\theta + C_{33}\sin^2\theta)\big]\varepsilon_{xx}\\ &+ \big[-2C_{44}^R\sin\theta\cos\theta(\cos^2\theta - \sin^2\theta)\\ &+ \sin\theta\cos\theta(C_{11}\cos^2\theta + C_{13}\sin^2\theta)\\ &- \cos\theta\sin\theta(C_{13}\cos^2\theta + C_{33}\sin^2\theta)\big]\gamma_{xz}\},\end{aligned} \tag{13}$$

$$\begin{aligned}\sigma_{xz} = (1 - i\omega\tau_R)\{&[(C_{11} - C_{13})\sin\theta\cos\theta\cos^2\theta\\ &-2C_{44}^R\sin\theta\cos\theta(\cos^2\theta - \sin^2\theta)\\ &+(C_{13} - C_{33})\sin^2\theta\sin\theta\cos\theta]\varepsilon_{xx}\\ &+\big[C_{44}^R(\cos^2\theta - \sin^2\theta)^2 + (C_{11} - C_{13})\sin^2\theta\cos^2\theta\\ &-(C_{13} - C_{33})\sin^2\theta\cos^2\theta\big]\gamma_{xz}\}.\end{aligned} \tag{14}$$

The bending moment M_x and shear force Q_x are determined as

$$M_x = \int_A \sigma_{xx} z\, dA, \tag{15}$$

$$Q_x = \int_A k_s\sigma_{xz} dA, \tag{16}$$

where A is the cross-sectional area of the beam and k_s is the shear correction factor depending on the shape of the cross section of the beam. Using the displacement components and stress components, Eq. (3) can be rewritten in the following form:

$$\begin{aligned}\frac{\partial\sigma_{xx}}{\partial x} + \frac{\partial\sigma_{xz}}{\partial z} &= \rho\frac{\partial^2\tilde{U}}{\partial t^2},\\ \frac{\partial\sigma_{xz}}{\partial x} + \frac{\partial\sigma_{zz}}{\partial z} &= \rho\frac{\partial^2\tilde{W}}{\partial t^2},\end{aligned} \tag{17}$$

where ρ is the mass density of the nematic elastomer. Integrating Eq. (17), we have

$$\int_A \frac{\partial\sigma_{xx}}{\partial x} z dA + \int_A \frac{\partial\sigma_{xz}}{\partial z} z dA = \int_A \rho\frac{\partial^2\tilde{U}}{\partial t^2} z dA, \quad \int_A \frac{\partial\sigma_{xz}}{\partial x} dA + \int_A \frac{\partial\sigma_{zz}}{\partial z} dA = \int_A \rho\frac{\partial^2\tilde{W}}{\partial t^2} dA. \tag{18}$$

Substitution of Eqs. (11), (15), and (16) into Eq. (18) leads to

$$\frac{\partial M_x}{\partial x} - Q_x = \rho I\frac{\partial^2\phi}{\partial t^2}, \quad \frac{\partial Q_x}{\partial x} = \rho A\frac{\partial^2 w}{\partial t^2}, \tag{19}$$

where I is the second moment of area. By making use of Eqs. (12)–(16), the equation of motion for the nematic elastomer Timoshenko beam is given as

$$\begin{aligned}&(1 - i\omega\tau_R)\big[4C_{44}^R\sin^2\theta\cos^2\theta + 2C_{13}\sin^2\theta\cos^2\theta + C_{11}\cos^4\theta + C_{33}\sin^4\theta\big]I\frac{\partial^2\phi}{\partial x^2} - (1 - i\omega\tau_R)k_s A\big[C_{44}^R(\cos^2\theta - \sin^2\theta)^2\\ &+ (C_{11} - 2C_{13} + C_{33})\sin^2\theta\cos^2\theta\big]\left(\frac{\partial w}{\partial x} + \phi\right) = \rho I\frac{\partial^2\phi}{\partial t^2},\\ &(1 - i\omega\tau_R)k_s A\big[C_{44}^R(\cos^2\theta - \sin^2\theta)^2 + (C_{11} - 2C_{13} + C_{33})\sin^2\theta\cos^2\theta\big]\left(\frac{\partial^2 w}{\partial x^2} + \frac{\partial\phi}{\partial x}\right) = \rho A\frac{\partial^2 w}{\partial t^2}.\end{aligned} \tag{20}$$

IV. THE NATURAL FREQUENCIES AND EIGENMODES OF THE NEMATIC ELASTOMER TIMOSHENKO BEAM

Assume that the displacement component has the form [27]

$$w = \sum_{m=1}^{\infty} e^{-i\omega_m t} W_m(x), \quad \phi = \sum_{m=1}^{\infty} e^{-i\omega_m t}\psi_m(x), \tag{21}$$

where ω_m ($m = 1,2,3,\ldots$) is a complex frequency, and $W_m(x)$ and $\psi_m(x)$ are complex functions to be determined which are the mth mode functions of the transverse displacement and the rotation.

Substitution of Eqs. (7) and (21) into Eq. (20) yields

$$(1-i\omega_m\tau_R)\left\{4\left[2c_5-\frac{d_2^2}{4d_1}\frac{(1-i\omega_m\tau_2)^2}{(1-i\omega_m\tau_1)(1-i\omega_m\tau_R)}\right]\sin^2\theta\cos^2\theta+2C_{13}\sin^2\theta\cos^2\theta+C_{11}\cos^4\theta+C_{33}\sin^4\theta\right\}I\frac{d^2\psi_m}{dx^2}$$
$$-(1-i\omega_m\tau_R)k_sA\left\{\left[2c_5-\frac{d_2^2}{4d_1}\frac{(1-i\omega_m\tau_2)^2}{(1-i\omega_m\tau_1)(1-i\omega_m\tau_R)}\right](\cos^2\theta-\sin^2\theta)^2+(C_{11}-2C_{13}+C_{33})\sin^2\theta\cos^2\theta\right\}$$
$$\times\left(\frac{dW_m}{dx}+\psi_m\right)=-\rho I\omega_m^2\psi_m,$$
$$(1-i\omega_m\tau_R)k_sA\left\{\left[2c_5-\frac{d_2^2}{4d_1}\frac{(1-i\omega_m\tau_2)^2}{(1-i\omega_m\tau_1)(1-i\omega_m\tau_R)}\right](\cos^2\theta-\sin^2\theta)^2+(C_{11}-2C_{13}+C_{33})\sin^2\theta\cos^2\theta\right\}\left(\frac{d^2W_m}{dx^2}+\frac{d\psi_m}{dx}\right)$$
$$=-\rho A\omega_m^2W_m. \tag{22}$$

Introduce a series of dimensionless coordinates and parameters, which are given in Appendix A. Equation (22) is then rewritten as the following dimensionless form, that is,

$$\left[4\lambda_1(1-i\Omega_m\tau_R')-\beta_1\frac{(1-i\Omega_m\tau_2')^2}{1-i\Omega_m\tau_1'}+g_1(1-i\Omega_m\tau_R')+2g_2(1-i\Omega_m\tau_R')+g_3(1-i\Omega_m\tau_R')\right]\frac{d^2\bar\psi_m}{d\xi^2}$$
$$-\left[\lambda_2(1-i\Omega_m\tau_R')-\frac{1}{4}\beta_2\frac{(1-i\Omega_m\tau_2')^2}{1-i\Omega_m\tau_1'}+\zeta(1-i\Omega_m\tau_R')\right]\left(\frac{d\bar W_m}{d\xi}+\bar\psi_m\right)=-g_4\Omega_m^2\bar\psi_m,$$
$$\left[\lambda_2(1-i\Omega_m\tau_R')-\frac{1}{4}\beta_2\frac{(1-i\Omega_m\tau_2')^2}{1-i\Omega_m\tau_1'}+\zeta(1-i\Omega_m\tau_R')\right]\left(\frac{d^2\bar W_m}{d\xi^2}+\frac{d\bar\psi_m}{d\xi}\right)=-\alpha\Omega_m^2\bar W_m\,. \tag{23}$$

Uncoupling Eq. (23) yields the following ordinary differential equation in the variable $\bar W_m$, that is,

$$A_1\frac{d^4\bar W_m}{d\xi^4}+B_1\frac{d^2\bar W_m}{d\xi^2}+C_1\bar W_m=0\,, \tag{24}$$

where A_1, B_1, and C_1 are given in Appendix B. In addition, α, β_1, β_2, g_1, g_2, g_3, g_4, and ζ in Appendix A are related to the chain anisotropic parameter r. When r tends to 1, NEs are degenerated to isotropic viscoelastic solid (Fig. 1), and the governing equation of motion is reduced to

$$-(1-i\Omega_m\tau_R')^2g_4\frac{d^4\bar W_m}{d\xi^4}-g_4\Omega_m^2(1-i\Omega_m\tau_R')(\alpha+1)$$
$$\times\frac{d^2\bar W_m}{d\xi^2}+\left[\alpha(1-i\Omega_m\tau_R')\Omega_m^2-\alpha g_4\Omega_m^4\right]\bar W_m=0. \tag{25}$$

Here we consider the hinged-hinged boundary condition, which means that both ends of the beam are restrained by hinged support. Because the hinged support only restrains the displacement and bending moment, it demands

$$\bar W_m(0)=\bar W_m(1)=\bar\psi_m'(0)=\bar\psi_m'(1)=0. \tag{26}$$

The numerical solution procedure of Eq. (24) is presented in Appendix C. Then we can obtain the dimensionless natural frequency f_m and decrement coefficient s_m. Correspondingly, $\bar W_m(\xi)$ and $\bar\psi_m(\xi)$ are the mth dimensionless mode functions of the transverse displacement and the rotation. Generally, both $\bar W_m(\xi)$ and $\bar\psi_m(\xi)$ are complex. The complex modal functions imply that the phase of the response is not a constant and thus the material particles of the NE beam do not pass through equilibrium simultaneously.

V. NUMERICAL RESULTS

In this section, the natural frequencies and decrement coefficients of a hinged-hinged NE beam are considered. In order to verify the validity of the present formulation, we first consider the situation that the nematic elastomer degenerates to the general isotropic viscoelastic solid by setting $r=1$. The parameters are chosen as $E=7\times10^9$ Pa, $G=2.6923\times10^9$ Pa, $\tau_R=1.069\times10^{-6}$ s, $\rho=2000\,\mathrm{kg\,m^{-3}}$, $L=0.4$ m, $L/h=7$, $k_s=5/6$ [27]. The first ten natural frequencies and decrement coefficients of a hinged-hinged nematic elastomer beam is calculated and compared with the results given by Chen *et al.* [27] for a pure viscoelastic Timoshenko beam.

Figure 4 shows that excellent agreement of the results is obtained, which verifies the suitability and reliability of the present solution method in the analysis of the free vibration characteristic equations of the hinged-hinged nematic elastomer Timoshenko beam.

Based on the above method, the natural frequencies and the corresponding decrement coefficients of a hinged-hinged nematic elastomer Timoshenko beam are calculated. Unless otherwise stated, the parameters for NEs used in the calculation are from Ref. [15]: $c_1=2c_2=2c_4=\mu_0=5\times10^5\,\mathrm{N\,m^{-2}}$, $c_3=5\times10^8\,\mathrm{N\,m^{-2}}$, $c_5=\mu_0(r+1)^2/8r$, $d_1=\mu_0(r-1)^2/r$, $d_2=\mu_0(1-r^2)/r$, $\rho=10^3\,\mathrm{kg\,m^{-3}}$, $\tau_1=10^{-2}$ s, $\tau_2=0.5\times10^{-4}$ s, $\tau_R=10^{-5}$ s. The length of the nematic elastomer beam is $L=0.4$ m, the thickness is $h=0.04$ m, and shear correction factor is $k_s=5/6$.

Internal relaxation of nematic directors leads to the dynamic softening of NEs. The dimensionless director rotation times τ_1' and τ_2' are two important parameters. The variations of the first and fourth order dimensionless natural frequencies

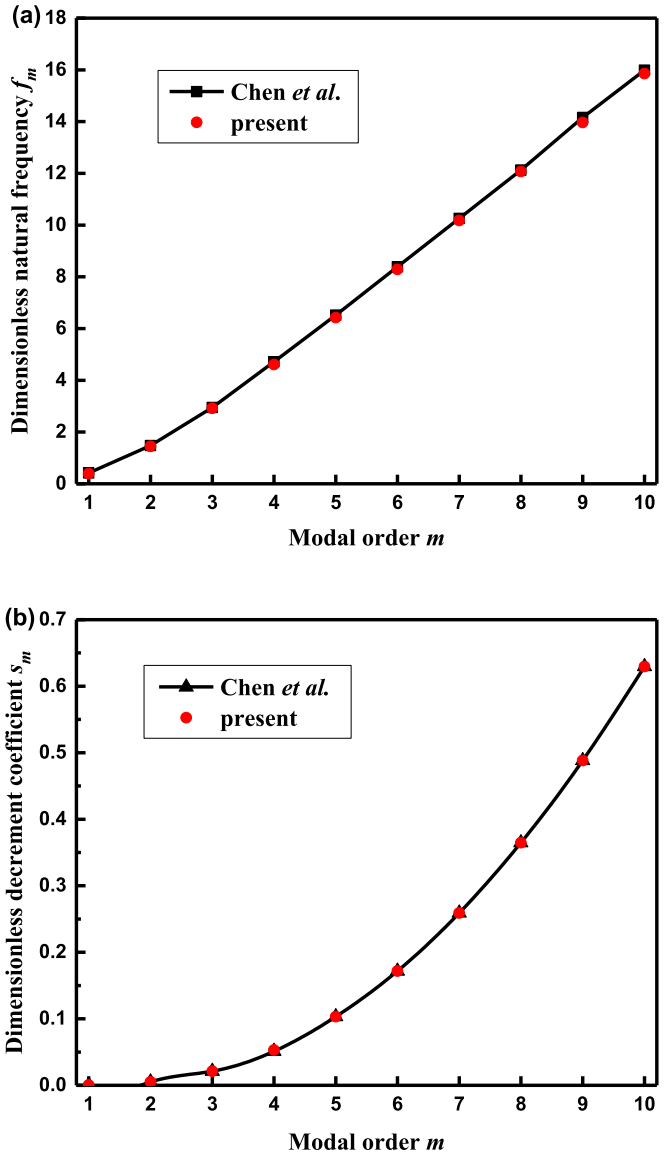

FIG. 4. Comparison of (a) the dimensionless natural frequencies; (b) decrement coefficients obtained by the present model and those given in Ref. [27].

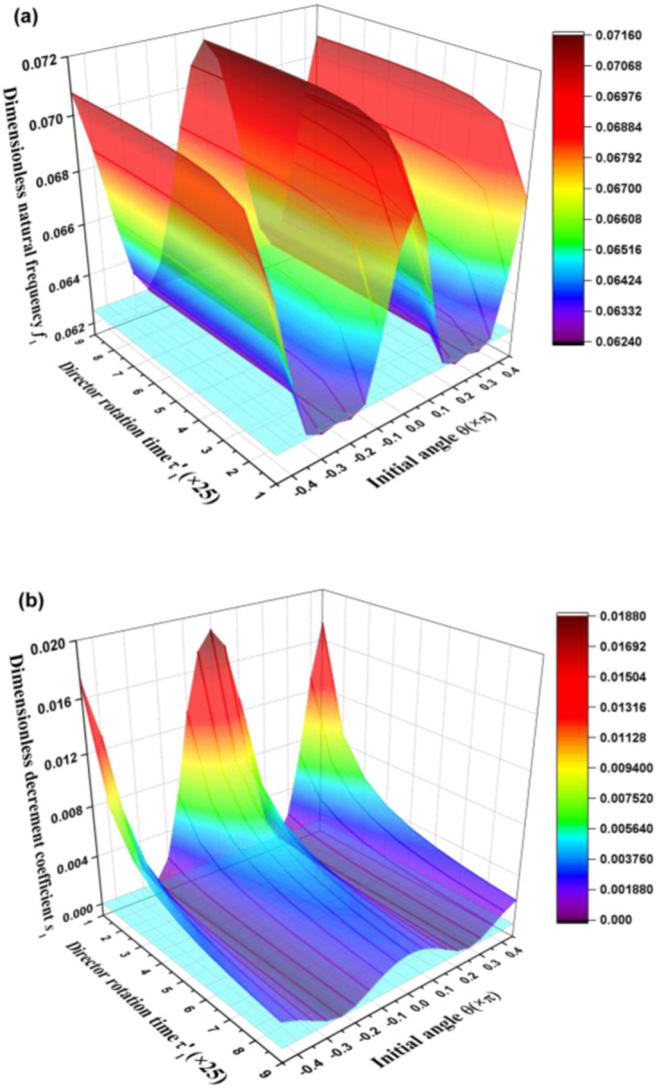

FIG. 5. The effect of τ_1' on the first-order (a) dimensionless frequencies and (b) decrement coefficients with $r = 3$, $\tau_2 = 0.5 \times 10^{-4}$ s, $\tau_R = 10^{-5}$ s (the cyan part corresponding to $r = 1$; the color coding shows the corresponding values).

and decrement coefficients with respect to τ_1' are given in Figs. 5 and 6, respectively. In the calculation, we have $r = 3$ (anisotropic case) and $r = 1$ (isotropic case). The cyan part corresponds to $r = 1$, i.e., the isotropic viscoelastic solid with no director relaxation. In this situation, the dimensionless natural frequency and decrement coefficient are independent of the dimensionless director rotation time τ_1' and initial angle θ, and the cyan part is a flat surface. When $r \neq 1$, as shown in Figs. 5 and 6, the natural frequencies increase slightly with the increasing of dimensionless director rotation time τ_1', while the decrement coefficients decrease dramatically at first, then slowly, and finally tend to a constant value along with the increase of τ_1'. At the higher eigenmode, the natural frequencies are less affected by τ_1', while the director rotation time has an obvious effect on the dissipation. It is easy to find that the director initial angle θ has a significant influence on the natural frequencies and decrement coefficients. The natural frequencies and decrement coefficients are symmetric to the initial angle and change periodically along with the variation of θ. The variation of natural frequencies and decrement coefficients presents a V mode when θ is among 0 to $\pi/2$, which means it decreases first to a minimum value and then increases with the increasing of θ. However, it is noticed that the variation of the first-order natural frequency with respect to the director initial angle θ presents a W mode when $\tau_1' < 2 \times 25$, with the values of the first-order frequencies less than those when $r = 1$, and the decrement coefficients greater than those when $r = 1$. Different from the V mode, it appears that there are four θ leading to a same natural frequency for a certain τ_1'. In addition, they have different decrement coefficients. This is due to the dynamic soft elasticity of NEs. When $\theta = \pi/4$, the natural frequency of the NE beam closes to the transition frequency from liquid crystal response to rubber response (Fig. 2). The deviation of θ from $\theta = \pi/4$ may cause the variation of $\mathrm{Im}(C_{44}^R)$ cross the transition frequency and have

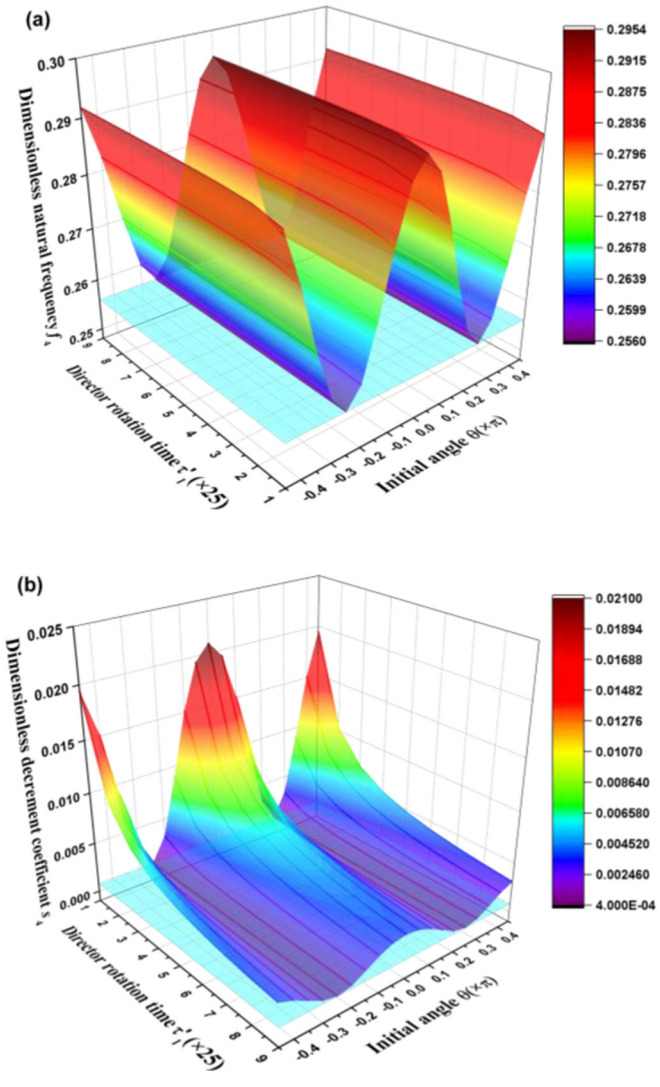

FIG. 6. The effect of τ_1' on the fourth-order (a) dimensionless frequencies and (b) decrement coefficients with $r = 3$, $\tau_2 = 0.5 \times 10^{-4}$ s, $\tau_R = 10^{-5}$ s (the cyan part corresponding to $r = 1$; the color coding shows the corresponding values).

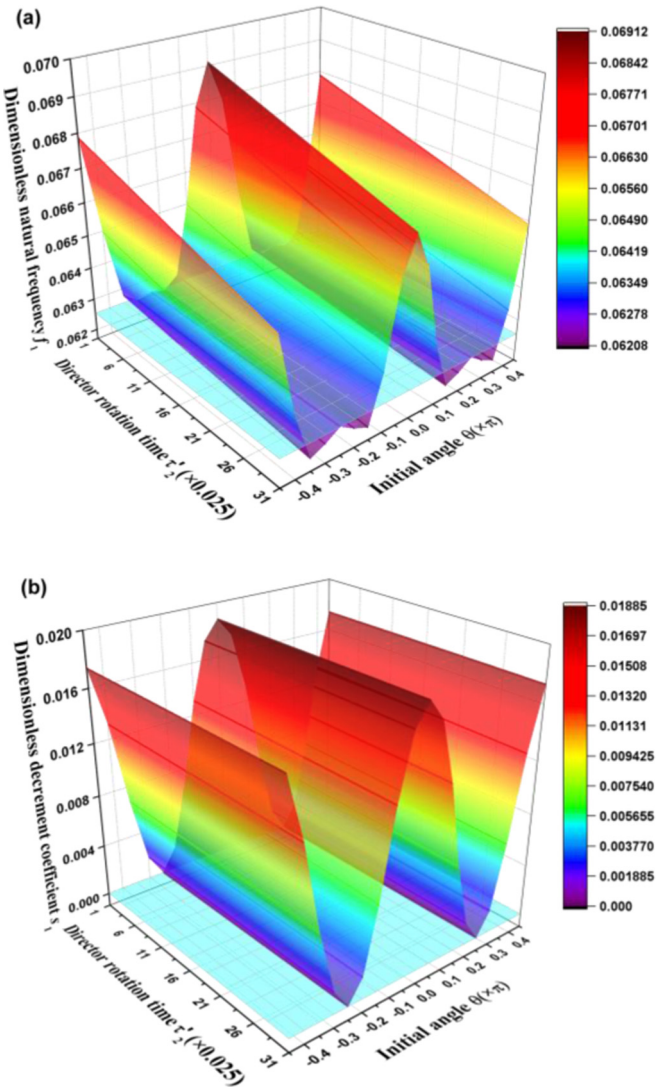

FIG. 7. The effect of τ_2' on the first-order (a) dimensionless frequencies and (b) decrement coefficients with $r = 3$, $\tau_1 = 10^{-2}$ s, $\tau_R = 10^{-5}$ s (the cyan part corresponding to $r = 1$; the color coding shows the corresponding values).

the same values at different frequencies near the transition one, which leads to the W mode near $\theta = \pi/4$. When the natural frequencies of NE beams are away from the transition frequency, it would be the V mode. The mode variation due to the dynamic soft elasticity of NEs would benefit the vibration analysis of NE beams near the transition frequency. For the fourth-order frequencies and decrement coefficients, they are all greater than those when $r = 1$. This can be explained from Fig. 2; that is, the real part of C_{44}^R increases relatively slowly with the frequency at a small τ_1'. Then the wider the frequency range in which the real part of C_{44}^R is smaller than that when $r = 1$ is, the smaller the natural frequency is, which is due to smaller storage modulus. In the same way, since the imaginary part of C_{44}^R is zero when $r = 1$, the absolute value of the imaginary part of C_{44}^R is always nonzero when $r \neq 1$, and the decrement coefficients are greater than that when $r = 1$. Moreover, the effect of τ_1' on the frequencies and decrement coefficients is evident for all modal orders and not given here anymore.

Figures 7 and 8 show the effect of dimensionless director rotation time τ_2' and the director initial angle θ on the dimensionless natural frequencies and decrement coefficients of NE beams. It can be seen that the natural frequencies are decreased with the increase of the director rotation time τ_2' for both of the lower and higher eigenmodes. When $r = 1$, the dimensionless natural frequency and decrement coefficient are independent of the dimensionless director rotation time τ_2' and initial angle θ, and the cyan part is a flat surface. As shown in Fig. 7(a), the variation of the first-order natural frequencies with respect to the director initial angle θ presents a W mode for all of τ_2' while θ is among 0 to $\pi/2$, and the values at the middle vertex equal those when $r = 1$. At the fourth eigenmode, the natural frequencies and decrement coefficients are generally greater than those when $r = 1$, and display V mode with the variation of the director initial angle, reaching the minimum values at $\theta = \pi/4$. With the increasing of τ_2', the first eigenmode of the decrement coefficients is less

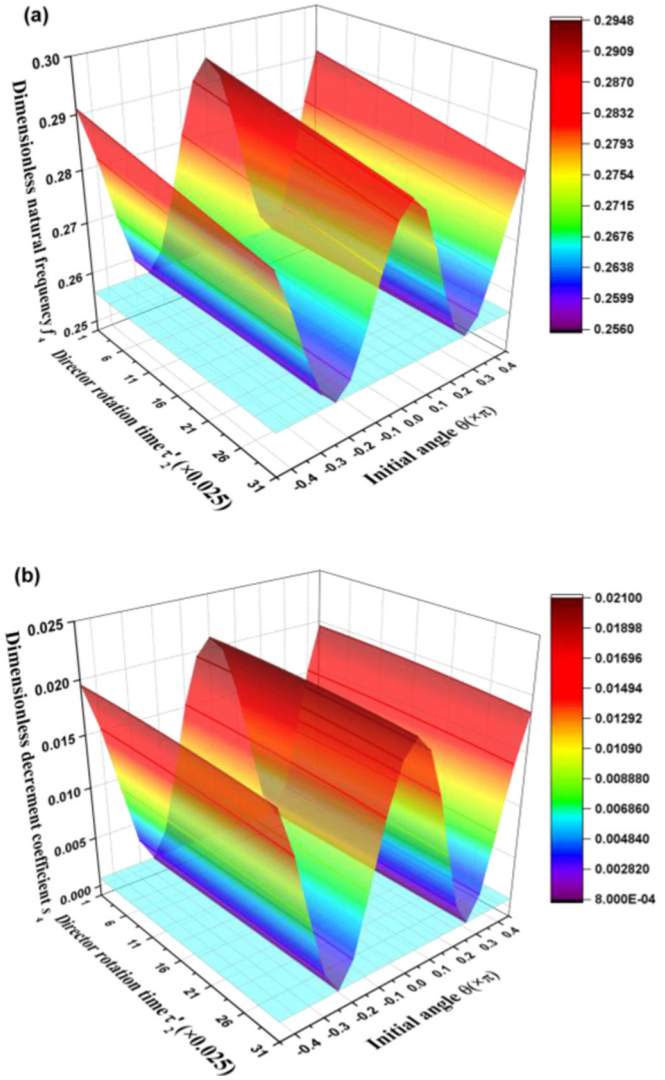

FIG. 8. The effect of τ_2' on the fourth-order (a) dimensionless frequencies and (b) decrement coefficients with $r = 3$, $\tau_1 = 10^{-2}$ s, $\tau_R = 10^{-5}$ s (the cyan part corresponding to $r = 1$; the color coding shows the corresponding values).

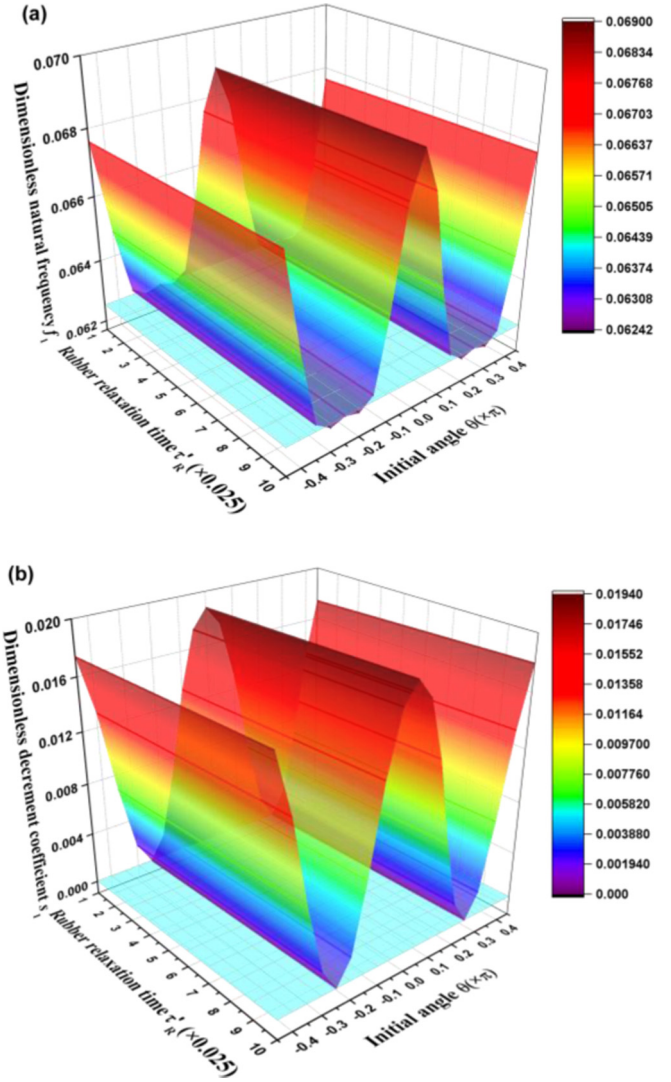

FIG. 9. The effect of τ_R' on the first-order (a) dimensionless frequencies and (b) decrement coefficients with $r = 3$, $\tau_1 = 10^{-2}$ s, $\tau_2 = 0.5 \times 10^{-4}$ s (the cyan part corresponding to $r = 1$; the color coding shows the corresponding values).

affected, whereas it decreases slightly at the fourth eigenmode, indicating that the higher the order of the eigenmode is, the more significantly the decrement coefficients are affected by τ_2'. Moreover, it shows that τ_2' plays a relatively greater role than τ_1' in the parameter study of NEs.

The influence of the dimensionless rubber relaxation time τ_R' and the director initial angle θ on the dimensionless natural frequencies and decrement coeffcients is plotted in Figs. 9 and 10, respectively. It can be seen from Figs. 9 and 10 that dimensionless rubber relaxation time τ_R' has fewer effects on the natural frequencies, whereas the decrement coefficients increase linearly. And the higher the modal order is, the more significantly the decrement coefficients are increased with the increase of τ_R'. This agrees well with the behavior of general isotropic viscoelastic beams. NEs possess the characteristics of general isotropic materials. It is noticed that the rubber relaxation time τ_R' has great effects on the dissipation of NE beams when $r = 1$, which is less affected by the director rotation time τ_1' and τ_2'. When $r > 1$, the variation of the natural frequencies and decrement coefficients present a V mode while θ varies from 0 to $\pi/2$ with larger values than those at $r = 1$. However, at the first eigenmode, the variation of natural frequencies also displays a W mode with a small middle vertex value equal to that when $r = 1$.

From the results above we can see that the chain anisotropic parameter has great effects on the natural frequencies and decrement coefficients of NE beams. In order to clearly manifest the influence of r, Fig. 11 gives the dimensionless natural frequencies and the decrement coefficients at different eigenmodes. Here $L = 0.6$ m is used to obtain lower natural frequencies. In the calculation we have $\tau_1 = 10^{-2}$ s, $\tau_2 = 0.5 \times 10^{-4}$ s, $\tau_R = 10^{-5}$ s. In Fig. 11, the natural frequencies increase linearly with the increasing of modal order m, and the larger the value of r is, the larger the slope is. It is noticed that the decrement coefficients have a sudden increase when the anisotropic parameter r is bigger than 1, which is due

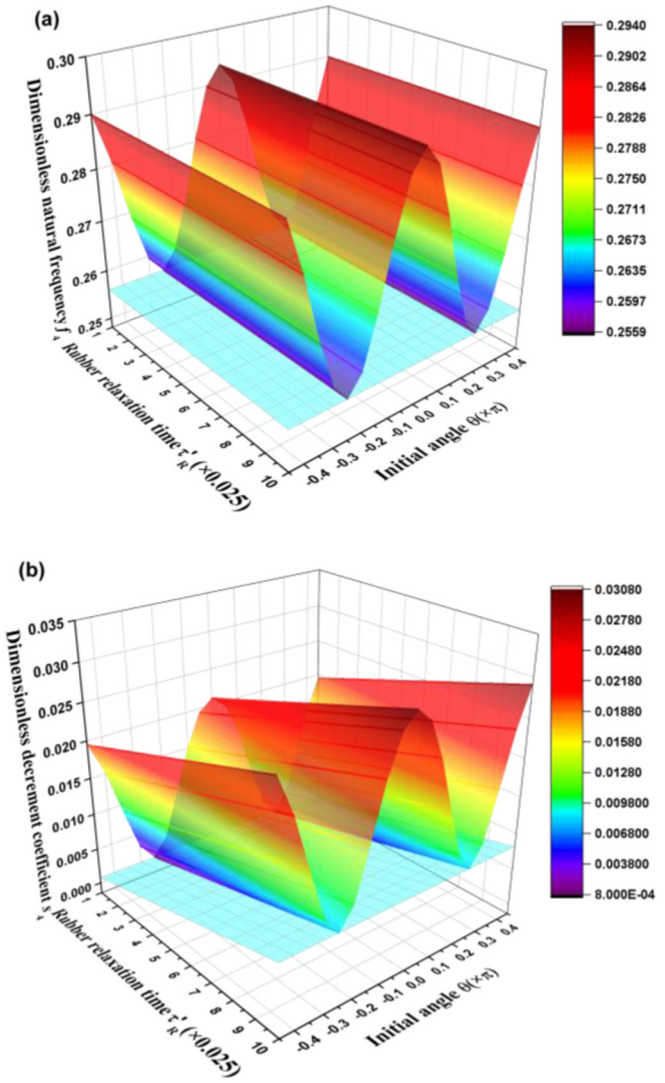

FIG. 10. The effect of τ'_R on the fourth-order (a) dimensionless frequencies and (b) decrement coefficients with $r = 3$, $\tau_1 = 10^{-2}$ s, $\tau_2 = 0.5 \times 10^{-4}$ s (the cyan part corresponding to $r = 1$; the color coding shows the corresponding values).

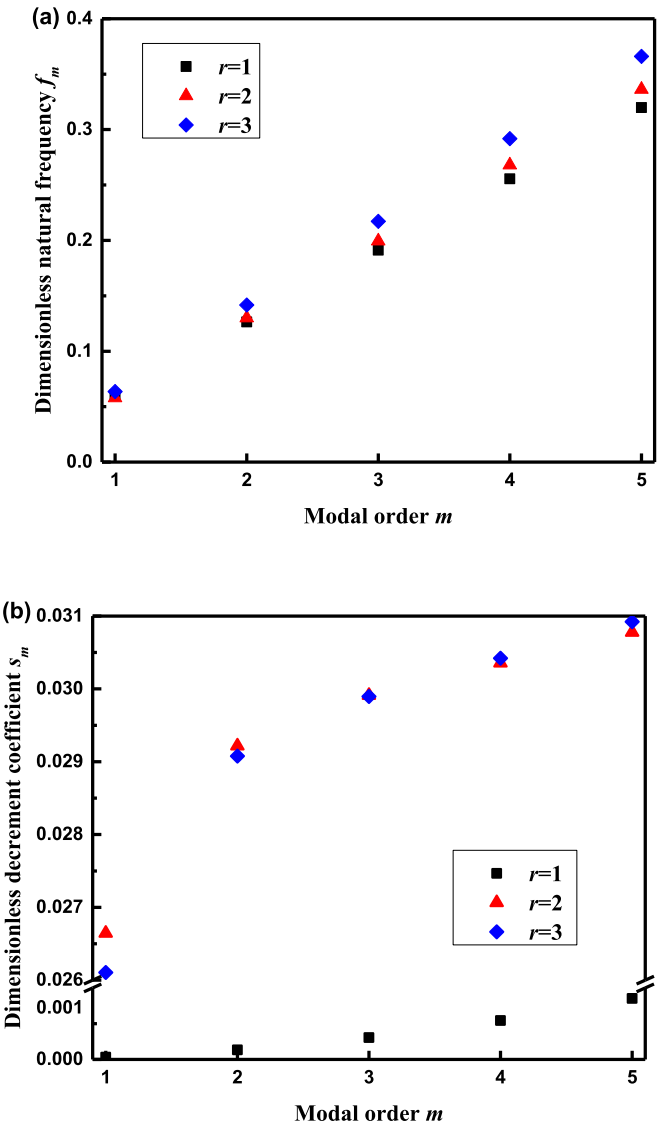

FIG. 11. The first five dimensionless (a) natural frequencies and (b) decrement coefficients with different chain anisotropic parameter r when $\tau_1 = 10^{-2}$ s, $\tau_2 = 0.5 \times 10^{-4}$ s, $\tau_R = 10^{-5}$ s.

to the transition from isotropic viscoelasticity ($r = 1$ with no director relaxation) to anisotropic viscoelasticity ($r > 1$ with shear flow and director relaxation). It is also seen that at higher eigenmode, the decrement coefficients increase slightly along with the increasing of r, whereas at the lower modal order, the decrement coefficients decrease with the increasing of r, which is due to the dynamic soft elasticity in a low-frequency limit for NEs.

In order to see clearly this variation due to the dynamic soft elasticity, Fig. 12 gives the first five decrement coefficients versus corresponding natural frequencies with different r. The symbols represent the decrement coefficients at the eigenfrequencies. Comparison with Fig. 2(b) reveals that the transform of C_{44}^R from liquid crystal response to rubber performance with respect to the frequency causes the slope variation of the decrement coefficients. Before NEs reach a rubber plateau, the greater the r is, the smaller the decrement coefficients at the eigenfrequencies are. The decrement coefficients have larger slopes due to the variation slope of C_{44}^R with respect to the frequency. Near the critical frequency at which NEs transform to a rubber response, the NE beams with different r have almost the same decrement coefficients at the eigenfrequencies, which is due to the independence of the critical transition frequency on the anisotropic parameter. Along with the further increase of the frequency, the slope becomes stable, and larger r corresponds to larger decrement coefficients at the eigenfrequencies, which is caused by larger absolute values of imaginary parts of C_{44}^R at larger r. The variation of the decrement coefficients reflects that the dynamic soft elasticity has distinct effects on the dissipation of the NE beams.

The real and imaginary parts of the modal functions of the NE Timoshenko beam with hinged-hinged ends at the first and fourth eigenmodes are shown in Fig. 13. It is found that the real and imaginary parts of the modal functions are almost the same in value but opposite in sign, and the amplitudes of the higher modal functions are smaller than

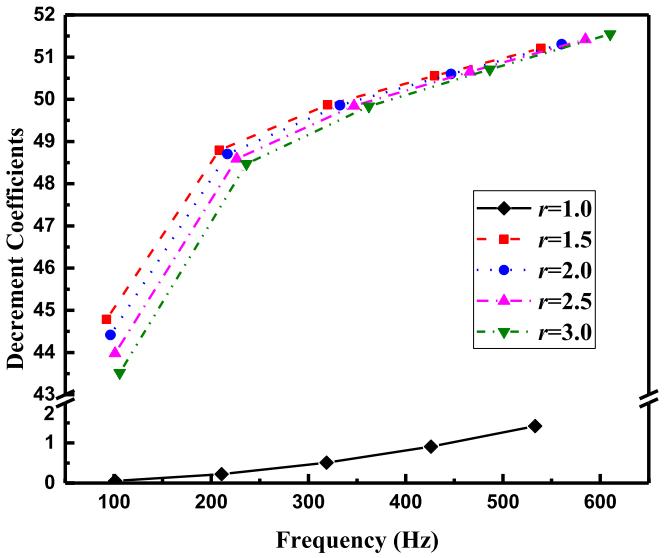

FIG. 12. The variation of decrement coefficients of the first five eigenmodes with respect to natural frequencies for NE beams with differernt anisotropic parameter r.

those of lower modal functions. The amplitude of the NE beam with $r > 1$ is bigger than that in the isotropic viscoelastic state ($r = 1$), which means that the nematic elastomers have a better deformation capability than ordinary isotropic viscoelastic materials, because the NEs have additional rotational degrees of freedom and display dynamic soft elasticity.

In order to manifest the influence of the director initial angle on the model functions, Fig. 14 shows the variation of the modal functions with respect to the director initial angle θ. For convenience, only the real parts of the first and fourth order modal functions of NEs beam are plotted. The results show that the amplitudes are decreased first and then increased with the increase of θ. The amplitudes have minimal values when the director initial angle θ is about $\pi/4$. This is because in this situation the principal stress direction is along $\pi/4$, that is, the direction of the director. So the director has little rotation, and the deformation capability is weakened.

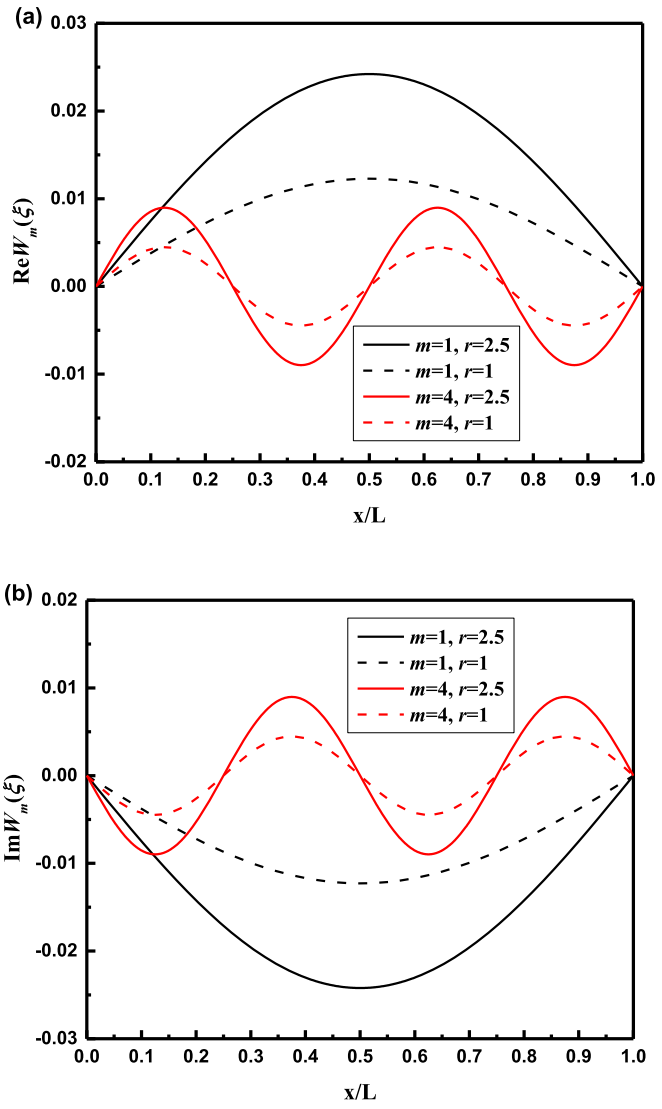

FIG. 13. (a) The real part and (b) the imaginary part of the first and fourth order modal functions of NE Timoshenko beam with hinged-hinged ends with $\tau_1 = 10^{-2}$ s, $\tau_2 = 10^{-4}$ s, $\tau_R = 10^{-6}$ s.

VI. CONCLUSIONS

This paper investigates the transverse vibration of a nematic elastomer beam based on the linear viscoelasticity theory and the Timoshenko beam model. The purpose is to master the vibration regularity so that we can prevent the damage of vibration and make better use of NE beam. The results show that the dynamic performance of the nematic elastomer beams is obviously different from general isotropic viscoelastic ones, whose dissipation only depends on the rubber relaxation time. For NE beams, the director dissipation and rotation have significant effects on their performance. Nematic elastomers have a better deformation capability than ordinary isotropic viscoelastic materials. Summarizing the results above we conclude the following:

(1) Director relaxation has great effects on the vibration of NE beams. The NE has its unique features by director rotation rather than general isotropic material. Along with the increase of τ_1', the natural frequency of the NE beam is increased with decreased dissipation coefficients. But the influence becomes weak at higher eigenmodes. However, along with the increase of τ_2', the natural frequency is decreased and the dissipation is less affected. The effects of the rubber relaxation time τ_R' on the natural frequencies are small, but the dissipation is greatly increased along with the increase of τ_R' at higher eigenmodes.

(2) The chain anisotropic parameter r has great effects on the natural frequencies and decrement coefficients of NE beams. When $r = 1$, NE beams degenerate to general viscoelastic ones, and the director relaxation has less effect on its vibration. But the dissipation is increased linearly along with the increase of rubber relaxation time. When $r \neq 1$, the natural frequencies and the values of vibration amplitude increase with the increase of r, and the decrement coefficients have a sudden increase due to the variation from isotropic viscoelasticity to anisotropic viscoelasticity. The slope of decrement coefficient versus frequency is larger for bigger r since the nematic elastomers display dynamic soft elasticity

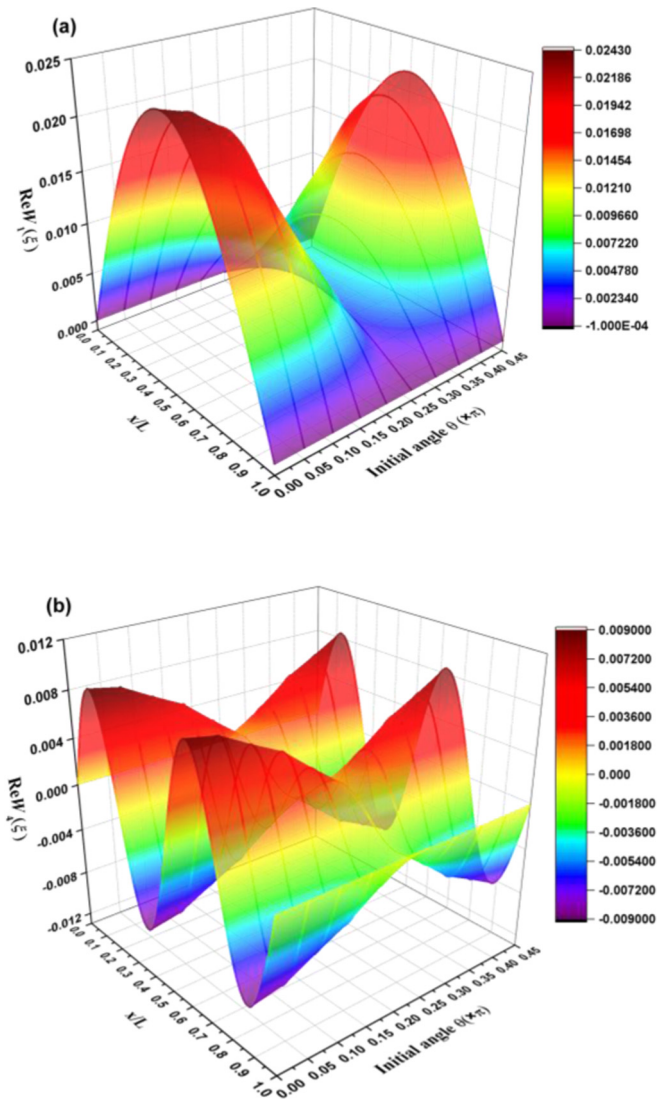

FIG. 14. The effect of director angle on the real parts of (a) the first and (b) fourth order modal functions of NE Timoshenko beam with hinged-hinged ends with $\tau_1 = 10^{-2}$ s, $\tau_2 = 10^{-4}$ s, $\tau_R = 10^{-6}$ s; the color coding shows the corresponding values.

at low frequency. Near the frequency at which NEs reach a rubber plateau, NE beams with different r have almost the same decrement coefficients at the eigenfrequencies, which is due to the independence of the transition frequency on the anisotropic parameter.

(3) The director initial angle θ also has great influence on the dynamic properties of NE beams. Both the natural frequencies and decrement coefficients present a periodical V mode with the increasing of director initial angle θ. However, in the first eigenmode, the variation of natural frequencies with respect to θ presents a periodical W mode while $\tau_1' < 2 \times 25$. The vibration amplitudes change periodically with respect to θ. The amplitudes of NE beams are first decreased and then increased along with the increase of the director initial angle, achieving the minimal value at $\theta = \pi/4$. These theoretical foundations are of great significance for the design of NEs especially for when we utilize or prevent the resonance of NE structure. By adjusting the director initial angle of the NE beam, we can control the natural frequency, decrement coefficient, and vibration amplitude of the NE beam.

The above results clarify the influence of intrinsic parameters of NEs on the dynamic properties of NE beams. Considering the availability of property controlling through external stimuli, the sensitivity of dynamic performance of NE beams to director initial angle and relaxation times provides a possibility of intelligent controlling of their dynamic performance.

ACKNOWLEDGMENTS

The second author acknowledges support from the Fundamental Research Funds for the Central Universities of China (Grant No. 2014JBZ014). Support from the National Natural Science Foundation of China (Grant No. 11272046) and National Basic Research Program of China (973 Program) (Grant No. 2015CB057800) is acknowledged.

APPENDIX A: DIMENSIONLESS COORDINATES AND PARAMETERS

The dimensional coordinates and parameters are defined as

$$\xi = \frac{x}{L}, \quad \bar{\psi}_m = \psi_m, \quad \bar{W}_m = \frac{W_m}{L}, \quad \tau_R' = \frac{\tau_R}{L}\sqrt{\frac{C_{11}}{\rho}},$$

$$\tau_1' = \frac{\tau_1}{L}\sqrt{\frac{C_{11}}{\rho}}, \quad \tau_2' = \frac{\tau_2}{L}\sqrt{\frac{C_{11}}{\rho}}, \quad \Omega_m = \omega_m L\sqrt{\frac{\rho}{C_{11}}},$$

$$\lambda_1 = \frac{I\sin^2\theta\cos^2\theta}{k_s A L^2}, \quad \lambda_2 = (\cos^2\theta - \sin^2\theta)^2, \quad \alpha = \frac{C_{11}}{2k_s c_5},$$

$$\beta_1 = \frac{d_2^2 I\sin^2\theta\cos^2\theta}{2k_s c_5 d_1 A L^2}, \quad \beta_2 = \frac{d_2^2(\cos^2\theta - \sin^2\theta)^2}{2c_5 d_1},$$

$$g_1 = \frac{C_{11} I\cos^4\theta}{2k_s c_5 A L^2}, \quad g_2 = \frac{C_{13} I\sin^2\theta\cos^2\theta}{2k_s c_5 A L^2}, \quad g_3 = \frac{C_{33} I\sin^4\theta}{2k_s c_5 A L^2},$$

$$g_4 = \frac{C_{11} I}{2k_s c_5 A L^2}, \quad \zeta = \frac{(C_{11} - 2C_{13} + C_{33})\sin^2\theta\cos^2\theta}{2c_5}. \tag{A1}$$

APPENDIX B: COEFFICIENTS A_1, B_1, AND C_1 IN EQ. (24)

The three coefficients A_1, B_1, and C_1 in Eq. (24) are derived as

$$A_1 = \left[4\lambda_1(1 - i\Omega_m\tau_R') - \beta_1\frac{(1 - i\Omega_m\tau_2')^2}{1 - i\Omega_m\tau_1'} + g_1(1 - i\Omega_m\tau_R') + 2g_2(1 - i\Omega_m\tau_R') + g_3(1 - i\Omega_m\tau_R')\right]$$
$$\times\left[\lambda_2(1 - i\Omega_m\tau_R') - \frac{1}{4}\beta_2\frac{(1 - i\Omega_m\tau_2')^2}{1 - i\Omega_m\tau_1'} + \zeta(1 - i\Omega_m\tau_R')\right], \tag{B1}$$

$$B_1 = \left[4\lambda_1(1-i\Omega_m\tau_2')-\beta_1\frac{(1-i\Omega_m\tau_2')^2}{1-i\Omega_m\tau_1'}+g_1(1-i\Omega_m\tau_R')+2g_2(1-i\Omega_m\tau_R')+g_3(1-i\Omega_m\tau_R')\right]\alpha\Omega_m^2$$
$$+g_4\left[\lambda_2(1-i\Omega_m\tau_R')-\frac{1}{4}\beta_2\frac{(1-i\Omega_m\tau_2')^2}{1-i\Omega_m\tau_1'}+\zeta(1-i\Omega_m\tau_R')\right]\Omega_m^2, \tag{B2}$$

$$C_1 = \alpha g_4\Omega_m^4-\alpha\left[\lambda_2(1-i\Omega_m\tau_R')-\frac{1}{4}\beta_2\frac{(1-i\Omega_m\tau_2')^2}{1-i\Omega_m\tau_1'}+\zeta(1-i\Omega_m\tau_R')\right]\Omega_m^2. \tag{B3}$$

APPENDIX C: THE SOLUTION PROCEDURE OF EQ. (24)

The characteristic equation of Eq. (24) is

$$A_1r_m^4+B_1r_m^2+C_1=0. \tag{C1}$$

Solving Eq. (C1), we have

$$r_{m1},r_{m2}=\pm\sqrt{\frac{-B_1+\sqrt{{B_1}^2-4A_1C_1}}{2A_1}},\quad r_{m3},r_{m4}=\pm\sqrt{\frac{-B_1-\sqrt{{B_1}^2-4A_1C_1}}{2A_1}}. \tag{C2}$$

Then the solution of the ordinary differential equation, Eq. (24), can be expressed as

$$\overline{W}_m(\xi)=C_{m1}(e^{\xi r_{m1}}+C_{m2}e^{\xi r_{m2}}+C_{m3}e^{\xi r_{m3}}+C_{m4}e^{\xi r_{m4}}). \tag{C3}$$

According to the relation between $\overline{W}_m(\xi)$ and $\overline{\psi}_m(\xi)$ in Eq. (23), the $\overline{\psi}_m(\xi)$ can be derived as

$$\overline{\psi}_m(\xi)=D_{m1}(e^{\xi r_{m1}}+D_{m2}e^{\xi r_{m2}}+D_{m3}e^{\xi r_{m3}}+D_{m4}e^{\xi r_{m4}}), \tag{C4}$$

where the relations between coefficients C_{mj} and D_{mj} are

$$D_{m1}=\frac{\alpha\Omega_m^2+Hr_{m1}^2}{-Hr_{m1}}C_{m1},\quad D_{mj}=\frac{\alpha\Omega_m^2+Hr_{mj}^2}{-D_{m1}Hr_{mj}}C_{m1}C_{mj}\quad (j=2,3,4),$$
$$H=\lambda_2(1-i\Omega_m\tau_R')-\frac{1}{4}\beta_2\frac{(1-i\Omega_m\tau_2')^2}{1-i\Omega_m\tau_1'}+\zeta(1-i\Omega_m\tau_R'). \tag{C5}$$

Combining Eq. (23) with Eq. (26), we have

$$\overline{W}_m(0)=0,\quad \overline{\psi}'_m(0)=p_m\overline{W}_m(0)-\overline{W}''_m(0)=0,$$
$$\overline{W}_m(1)=0,\quad \overline{\psi}'_m(1)=p_m\overline{W}_m(1)-\overline{W}''_m(1)=0, \tag{C6}$$

where

$$p_m=-\alpha\Omega_m^2/H. \tag{C7}$$

Substitution of Eq. (C3) into Eq. (C6) yields

$$\begin{bmatrix}1 & 1 & 1 & 1\\ e^{r_{m1}} & e^{r_{m2}} & e^{r_{m3}} & e^{r_{m4}}\\ B_{m1} & B_{m2} & B_{m3} & B_{m4}\\ B_{m1}e^{r_{m1}} & B_{m2}e^{r_{m2}} & B_{m3}e^{r_{m3}} & B_{m4}e^{r_{m4}}\end{bmatrix}\begin{bmatrix}1\\ C_{m2}\\ C_{m3}\\ C_{m4}\end{bmatrix}C_{m1}=0, \tag{C8}$$

where

$$B_{mj}=p_m-r_{mj}^2\quad (j=1,2,3,4). \tag{C9}$$

For the nontrivial solution of Eq. (C8), the determinant of the coefficient matrix must be zero, which leads to

$$(e^{r_{m1}}-e^{r_{m2}})(e^{r_{m3}}-e^{r_{m4}})(B_{m1}B_{m2}+B_{m3}B_{m4})+(e^{r_{m1}}-e^{r_{m3}})(e^{r_{m2}}-e^{r_{m4}})(-B_{m1}B_{m3}-B_{m2}B_{m4})$$
$$+(e^{r_{m2}}-e^{r_{m3}})(e^{r_{m1}}-e^{r_{m4}})(B_{m2}B_{m3}+B_{m1}B_{m4})=0. \tag{C10}$$

By numerically solving Eq. (C10), one can obtain the value of Ω_m, which is a complex number. Separation of the real and the imaginary parts of Ω_m gives $\Omega_m=-f_m-is_m$ $(m=1,2,3,\ldots)$, where f_m is the mth dimensionless natural frequency, and s_m the mth dimensionless decrement coefficient representing the speed of amplitude attenuation. Correspondingly, $\overline{W}_m(\xi)$ and

$\overline{\psi}_m(\xi)$ are the mth dimensionless mode functions of the transverse displacement and the rotation. And one can obtain the modal function of the hinged-hinged nematic elastomer beam as follows:

$$\begin{aligned}\overline{W}_m(\xi) = C_{m1}\Bigg\{ & e^{\xi r_{m1}} + \frac{e^{\xi r_{m2}}[(e^{r_{m4}} - e^{r_{m3}})B_{m1} + (e^{r_{m1}} - e^{r_{m4}})B_{m3} + (e^{r_{m3}} - e^{r_{m1}})B_{m4}]}{(e^{r_{m3}} - e^{r_{m4}})B_{m2} + (e^{r_{m4}} - e^{r_{m2}})B_{m3} + (e^{r_{m2}} - e^{r_{m3}})B_{m4}} \\ & + \frac{e^{\xi r_{m3}}[(e^{r_{m2}} - e^{r_{m4}})B_{m1} + (e^{r_{m4}} - e^{r_{m1}})B_{m2} + (e^{r_{m1}} - e^{r_{m2}})B_{m4}]}{(e^{r_{m3}} - e^{r_{m4}})B_{m2} + (e^{r_{m4}} - e^{r_{m2}})B_{m3} + (e^{r_{m2}} - e^{r_{m3}})B_{m4}} \\ & + \frac{e^{\xi r_{m4}}[(e^{r_{m3}} - e^{r_{m2}})B_{m1} + (e^{r_{m1}} - e^{r_{m3}})B_{m2} + (e^{r_{m2}} - e^{r_{m1}})B_{m3}]}{(e^{r_{m3}} - e^{r_{m4}})B_{m2} + (e^{r_{m4}} - e^{r_{m2}})B_{m3} + (e^{r_{m2}} - e^{r_{m3}})B_{m4}} \Bigg\}, \end{aligned} \tag{C11}$$

where C_{m1} can be obtained from the orthogonality condition of vibration mode functions:

$$\begin{aligned}\int_0^1 \Bigg\{ & \alpha\left(\Omega_n^2 - \Omega_m^2\right)\overline{W}_n(\xi)\overline{W}_m(\xi) + \left[g_4\left(\Omega_n^2 - \Omega_m^2\right) + i\tau_R'(\lambda_2 + \zeta)(\Omega_n - \Omega_m) + \frac{\beta_2}{4}\frac{(1 - i\Omega_n\tau_2')^2}{1 - i\Omega_n\tau_1'} - \frac{\beta_2}{4}\frac{(1 - i\Omega_m\tau_2')^2}{1 - i\Omega_m\tau_1'} \right] \\ & \times \bar{\psi}_n(\xi)\bar{\psi}_m(\xi) + \left[i\tau_R'(\lambda_2 + \zeta)(\Omega_n - \Omega_m) + \frac{\beta_2}{4}\frac{(1 - i\Omega_n\tau_2')^2}{1 - i\Omega_n\tau_1'} - \frac{\beta_2}{4}\frac{(1 - i\Omega_m\tau_2')^2}{1 - i\Omega_m\tau_1'} \right][\overline{W}_n{}'(\xi)\overline{W}_m{}'(\xi) - \overline{W}_m(\xi)\overline{\psi}_n{}'(\xi) \\ & + \overline{W}_n{}'(\xi)\bar{\psi}_m(\xi)] + \left[i\tau_R'(4\lambda_1 + g_1 + 2g_2 + g_3)(\Omega_n - \Omega_m) + \beta_1\frac{(1 - i\Omega_n\tau_2')^2}{1 - i\Omega_n\tau_1'} - \beta_1\frac{(1 - i\Omega_m\tau_2')^2}{1 - i\Omega_m\tau_1'} \right]\overline{\psi}_n{}'(\xi)\overline{\psi}_m{}'(\xi) \Bigg\} d\xi = 0. \end{aligned} \tag{C12}$$

[1] E. M. Terentjev, J. Phys.: Condens. Matter **11**, R239 (1999).
[2] H. R. Brand and H. Finkelmann, in *Handbook of Liquid Crystals Set*, edited by D. Demus *et al.* (Wiley VCH, New York, 1998).
[3] P. G. de Gennes and J. Prost, *The Physics of Liquid Crystals* (Oxford University Press, Oxford, 1995).
[4] H. Finkelmann, H. J. Kock, and G. Rehage, Makromolekulare Chemie, Rapid Communications **2**, 317 (1981).
[5] M. Warner and E. M. Terentjev, *Liquid Crystal Elastomers* (Clarendon Press, Oxford, 2003).
[6] L. Golubović and T. C. Lubensky, Phys. Rev. Lett. **63**, 1082 (1989).
[7] P. I. C. Teixeira and M. Warner, Phys. Rev. E **60**, 603 (1999).
[8] D. E. Carlson, E. Fried, and S. Sellers, J. Elasticity **69**, 161 (2002).
[9] S. M. Clarke, A. Hotta, A. R. Tajbakhsh, and E. M. Terentjev, Phys. Rev. E **65**, 021804 (2002).
[10] O. Stenull and T. C. Lubensky, Phys. Rev. E **69**, 051801 (2004).
[11] E. Terentjev and M. Warner, Eur. Phys. J. E **4**, 343 (2001).
[12] L. J. Fradkin, I. V. Kamotski, E. M. Terentjev, and D. D. Zakharov, Proc. R. Soc. London, Ser. A **459**, 2627 (2003).
[13] B. Singh, J. Phys. D: Appl. Phys. **40**, 584 (2007).
[14] D. Zakharov, Math. Mech. Solid. **17**, 67 (2011).
[15] S. Yang, Y. Liu, Y. Gu, and Q. Yang, Soft Matter **10**, 4110 (2014).
[16] L. Jin, X. Jiang, and Y. Huo, Sci. China, Ser. G: Phys., Mech. Astron. **49**, 553 (2006).
[17] L. Jin, Y. Yan, and Y. Huo, Int. J. Nonlinear Mech. **45**, 370 (2010).
[18] M. Warner, Phys. Rev. E **86**, 022701 (2012).
[19] M. Li, S. Lv, and J. Zhou, Smart Mater. Struct. **23**, 125012 (2014).
[20] Z. Ábrahám and G. Károlyi, Int. J. Nonlinear Mech. **70**, 126 (2015).
[21] N. An, M. Li, and J. Zhou, Smart Mater. Struct. **25**, 015016 (2016).
[22] K. Li and S. Cai, J. Appl. Mech. **83**, 031009 (2015).
[23] J. Schmidtke, W. Stille, and G. Strobl, Macromolecules **33**, 2922 (2000).
[24] M. Schönstein, W. Stille, and G. Strobl, Eur. Phys. J. E **5**, 511 (2001).
[25] R. W. Clough and J. Penzien, *Dynamics of Structures* (McGraw-Hill, New York, 1975).
[26] M. H. Li and P. Keller, Philos. Trans. R. Soc. London, Ser. A **364**, 2763 (2006).
[27] L.-Q. Chen, L. Peng, A.-Q. Zhang, and H. Ding, J. Vibrat. Control (2015).